ADVANCES IN ATMOSPHERIC SCIENCES, VOL. 22, NO. 1, 2005, 122–125

Interdecadal Variations of Phase Delays Between Two Niño Indices at Different Time Scales

BIAN Jianchun* (卞建春) and YANG Peicai (杨培才)

Institute of Atmospheric Physics, Chinese Academy of Sciences, Beijing 100029

(Received 25 November 2003; revised 31 March 2004)

ABSTRACT

Phase delays between two Niño indices—sea surface temperatures in Niño regions 1+2 and 3.4 (1950–2001)—at different time scales are detected by wavelet analysis. Analysis results show that there are two types of period bifurcations in the Niño indices and that period bifurcation points exist only in the region where the wavelet power is small. Interdecadal variation features of phase delays between the two indices vary with different time scales. In the periods of 40–72 months, the phase delay changes its sign in 1977: Niño 1+2 indices are 2–4 months earlier than Niño 3.4 indices before 1977, but 3–6 months later afterwards. In the periods of 20–40 months, however, the phase delay changes its sign in another way: Niño 1+2 indices are 1–4 months earlier before 1980 and during 1986–90, but 1–4 months later during 1980–83 and 1993–2001.

Key words: period bifurcations, different time scales, phase delay, interdecadal variation

1. Introduction

Since the late 1970s, the characteristics of ENSO have experienced notable changes (Wang, 1995). Rasmusson and Carpenter (1982) made a comprehensive description of a composite ENSO scenario based on six events during 1950–1976. The four Pacific basin-wide warming events (1982–83, 1986–87, 1991–95, 1997–98) after the late 1970s, however, appear to behave quite differently from the canonical scenario of Rasmusson and Carpenter (1982) (RC composite hereafter) (Wang, 1995; McPhaden, 1999). In the RC composite, the SST warm area first occurred over the South American coastal seas, and then expanded westward to the central tropical Pacific. In the last four warming events, however, the South American coastal warming as described in the RC composite did not precede the central Pacific warming. The aim of this work is to study how the phase relationship of the SST warming over different tropical Pacific areas, such as the South American coastal seas and the central tropic Pacific, changes with time.

It is well known that the periodicity of ENSO can be quite irregular, from 2 years to 7 years. The singular spectrum analysis–maximum entropy method and revised multitaper method show that two oscillatory modes, the low-frequency quasi-quadrennial mode (peaking at about 4.8–5.5 years) and the quasi-biennial mode (peaking at about 2.4–2.5 years), play essential roles in ENSO variability (Jiang et al., 1995; Ghil et al., 2002). For the low-frequency mode, an abrupt frequency shift was detected near 1960 (Wang and Wang, 1996; Moron et al., 1998; Yiou et al., 2000). Based on the monthly southern oscillation index for 1933–96, Yiou et al. (2000) concluded that the characteristic periodicity goes from about 5 years (during 1943–61) to roughly 3 years (during 1963–80). By using the Niño 3.4 SST anomaly, An and Wang (2000) found a notable transition of ENSO cycle frequency (from a relatively high to a relatively low frequency) in the late 1970s. For instance, a period of 20–30 months is dominant during 1962–67 while a period of 30–50 months is dominatnt during 1967–73, and an even longer period of 40–60 months is dominant from 1980 to the early 1990s. Because of the broad spectrum of the ENSO cycle, the present work will focus on how the phase delays between different Niño SST indices change at various time scales.

The analysis method used here is based on wavelet analysis, which is becoming a common tool for analyzing localized variations of power within a time series. By decomposing a time series into time–frequency

*E-mail: bjc@mail.iap.ac.cn

space, one is able to determine both the dominant modes of variability and how those modes vary in time (Torrence and Campo, 1998; Liu et al., 1995; Lin et al., 1999). The wavelet transform has been used to analyze the climatic hierarchy of different scales and the self-similarity of climatic jump points (Liu et al., 1995; Liu et al, 2000) and to predict the climate (Lin and Shi, 2003). Wavelet analysis was used to study the multi-scale fractal characteristics (Li et al., 2001) and the coherent structures in turbulent flows (Farge, 1992). Lin et al. (1999) used wavelet analysis to study the variation of dryness and wetness grades series in different levels and found that wavelet analysis can be used to detect the existence of phase differences in two areas. These research works show that the wavelet transform can be used to analyze time series that contain nonstationary power at many different frequencies and a phase difference between two time series at different scales. In section 2, the data and the analysis method will be introduced. The results will be given in section 3, and some conclusions will be drawn in the last section.

2. Data and analysis method

Two Niño SST indices, Niño 1+2 and Niño 3.4, will be used to study the phase relationship of the SST warming over different tropical Pacific areas. Niño 1+2 indices are defined as the monthly SST averaged over the eastern Pacific (0–10°S, 90°–80°W), while Niño 3.4 indices are over the central tropical Pacific (5°N–5°S, 170°–120°W). Data for 1950–2001 are from the Climate Prediction Center, the National Oceanic & Atmospheric Administration (CPC/NOAA). The base period (1971–2000) is used to calculate the monthly Niño region anomalies (http://www.cpc.ncep.noaa.gov/data/indices/).

Wavelet analysis is used to detect the phase delays between the two Niño SST indices. Here, the wavelet transform used in this article is briefly introduced. The detailed description can be found in Torrence and Compo (1998). The morlet wavelet is a complex wavelet function, which will return information about both amplitude and phase and is better adapted for capturing oscillatory behavior. So, here we use the Morlet wavelet with the non-dimensional frequency ω_0 taken to be 6. For the Morlet wavelet with ω_0=6, the relationship between the equivalent Fourier period λ and the wavelet scale s is λ=1.03 s.

3. Results

A continuous Morlet wavelet transformation is applied to Niño indices 1+2 and Niño 3.4 indices (1950–2001), and the results are shown in Fig. 1. From its variation with time, the wavelet power spectrum of the Niño 3.4 indices experiences significant changes during 1950–2001. During 1950–61, the power is larger than 5 above the period of 40 months, with the local extreme value near the period of 63 months. The power spectrum experiences an abrupt change in the early 1960s. In 1962, the region with the power larger than 5 is in the period range of 20–35 months, and then expands towards the longer period. During 1962–75, the local extreme points vary from the period of 30 months to 45 months. During 1979–91, the local extreme points vary little around the period of 57 months. This result is in accordance with An and Wang (2000). During 1992–99, the power spectrum bifurcates into two local extremes, one near the period of 60 months and another of 37 months.

Next, we can locate the period bifurcation points according to the zero real part of the wavelet transformation. It can be seen in Fig. 1 that there are two types of period bifurcations, which are illustrated in Fig. 2. For the first type, with the decrease of period length, the original solid (or vacant) dotted curve bifurcates at a point into three limbs, with the middle one turning vacant (or solid) while the side two remain unchanged, as we see in the two cases in Fig. 2a and b, respectively. The point where the bifurcation occurs is named the period bifurcation point, denoted by symbol "×". For the second type, however, with the decrease of period length, the original pair of solid-vacant dotted curves bifurcate at a pair of points into four limbs, solid-vacant-solid-vacant, respectively. The period bifurcation points occur in pairs as illustrated in Fig. 2c.

Between the periods of 40–60 months, there are in total 10 bifurcation points in the Niño 3.4 indices during 1950–2001. There are two cases of the first type (denoted by symbol "×" in Fig. 1), March 1952 (at the period of 42 months) and December 1993 (52 months). And there are four pairs of the second type (denoted by symbol "★"), December 1960 and February 1963 (42 months), April 1962 and March 1965 (58 months), October 1966 and April 1970 (69 months), and September 1976 and February 1979 (51 months). Similarly, in the period range of 20–40 months, the two types of bifurcation points can also be found. It is noticed that all but a few bifurcation points are located in the blank region with the wavelet power less than 5; that is to say, the period bifurcation only occurs in the region where the power of wavelet analysis is small. The same analysis for the Niño 1+2 indices also shows that the period bifurcation points only occur in the small power region of the wavelet analysis.

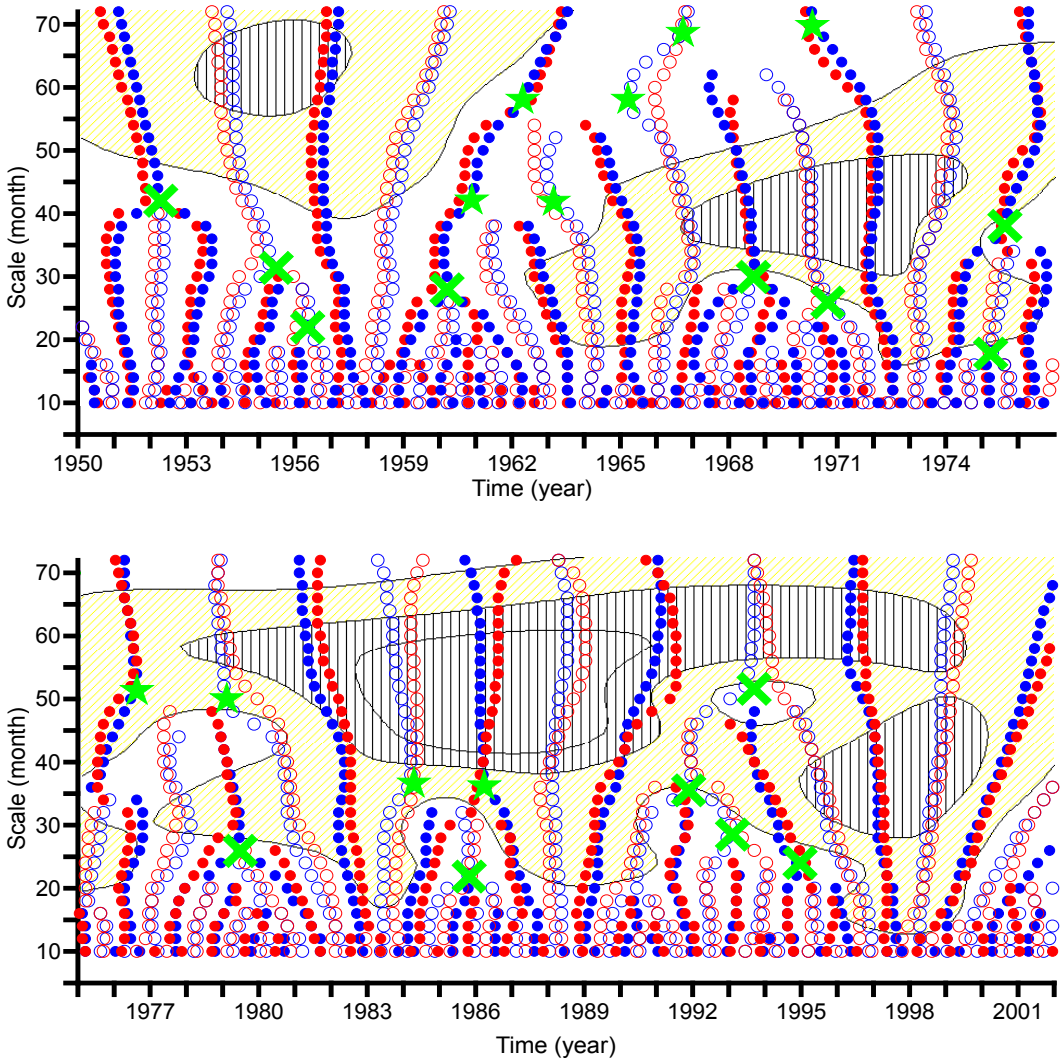

Fig. 1. The period bifurcation series of Niño 1+2 (red) and Niño 3.4 (blue) indices during 1950–2001. Dots denote the points where the real part of the wavelet transformation equals to zero, with the solid dots going from negative to positive with the increase of time at the same scale, and the vacant ones contrariwise. The shading shows the variation of the wavelet power spectrum of Niño 3.4 indices with time: the power is less than 5 in the blank area, in between (5 and 15) in the yellow area, and larger than 15 in the gray area.

Finally, we analyze the phase delays between the Niño 1+2 indices and Niño 3.4 indices at different timescales. The analysis above shows that the period bifurcation points occur in the small power region. In addition, Fig. 1 shows that the phase delays between the two Niño indices nearly keep invariable to the change of period length or at least keep the same sign, in the regions where the wavelet power of Niño 3.4 indices is larger than 5 (during the period of 20–40 months) or larger than 15 (during the period 40–72 months). Therefore, only these regions are considered when analyzing the phase delays, with no considerations given to the small power regions. It can be found in Fig. 1 that the temporal variation features of phase delays between the two indices vary with different time scales. In the period range of 40–72 months, the phase difference between the two Niño indices changes its sign in 1977: Niño 1+2 indices are about 2–4 months earlier than Niño 3.4 indices before 1977, and roughly 3–6 months later afterwards. That is to say, in the time scales of 40–72 months, the SST warming first occurred over the eastern Pacific, and 2–4 months later occurred over the central tropical Pacific before 1977, as described in the RC composite. After 1977, however, the SST warming occurred first over the central tropical Pacific, and 3–6 months later

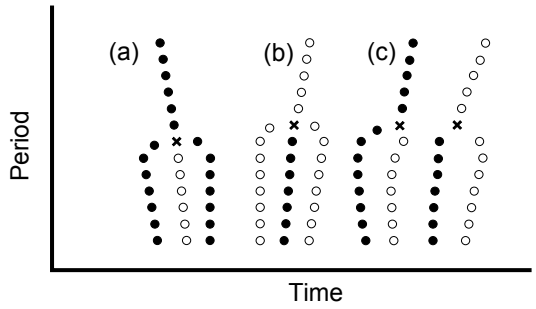

Fig. 2. Schematic diagram of locating the period bifurcation point (denoted by "×") based on the crossed curves of the real part of the wavelet transformation with value of zero (denoted by dots). (a) and (b) stand for the first kind and (c) for the second kind of period bifurcation.

over the eastern Pacific.

However, in the periods of 20–40 months, the phase delay changes its sign in another complex way: Niño 1+2 indices are about 1–4 months earlier than Niño 3.4 indices before 1980 and during 1986–90, but about 1–4 months later during 1980–83 and 1993–2001.

4. Summary

Morlet wavelet analysis is used here to detect phase delays between two Niño indices—Niño 1+2 and Niño 3.4 at different time scales. The analysis results seem to show that there are two types of period bifurcations in the Niño indices and that period bifurcation points exist only in the region where the wavelet power is small. The interdecadal variation features of phase differences between the two indices change with different time scales. In the periods of 40–72 months, the phase delay between the two indices changes its sign in 1977: Niño 1+2 indices are roughly 2–4 months earlier than Niño 3.4 indices before 1977, but about 3–6 months later after 1977. However, in the periods of 20–40 months, the phase delay changes its sign in another complex way: Niño 1+2 indices are about 1–4 months earlier than Niño 3.4 indices before 1980 and during 1986–90, but about 1–4 months later during 1980–83 and 1993–2001.

Acknowledgments. This work was supported by the National Natural Science Foundation of China under Grant No. 40035010.

REFERENCES

An, S. I., and B. Wang, 2000: Interdecadal changes in the structure of ENSO mode and their relation to changes of ENSO frequency. *J. Climate*, **13**, 2044–2055.

Farge, M., 1992: Wavelet transforms and their applications to turbulence. *Annual Review Fluid Mechanics*, **24**, 395–457.

Ghil, M., and Coauthors, 2002: Advanced spectral methods for climatic time series. *Rev. Geophys.*, **40**(1), 1003, doi:10.1029/2000RG000092.

Jiang, N., D. Neelin, and M. Ghil, 1995: Quasi-quadrennial and quasi-biennial variability in the equatorial Pacific. *Climate Dyn.*, **12**, 101–112.

Li Xin, Hu Fei, Liu Gang, and Hong Zhongxiang, 2001: Multi-scale fractal characteristics of atmospheric boundary turbulence. *Adv. Atmos. Sci.*, **18**(5), 787–792.

Lin Zhenshan, and Shi Xiangsheng, 2003: The decade-scale climatic forecasting in China. *Adv. Atmos. Sci.*, **20**(4), 604–611.

Lin Zhenshan, Bian Weilin, Jin Long, and Yue Qun, 1999: Level analysis of dryness and wetness grades series. *Acta Meteorologica Sinica*, **57**(1), 112–120. (in Chinese)

Liu Shida, Rong Pingping, and Chen Jiong, 2000: The hierarchical structure of climate series. *Acta Meteorologica Sinica*, **58**(1), 110–114. (in Chinese)

Liu Taizhong, Rong Pingping, Liu Shida, Zheng Zuguang, and Liu Shikuo, 1995: Wavelet analysis of climate jump. *Acta Meteorologica Sinica*, **38**(2), 158–162. (in Chinese)

McPhaden, M. J., 1999: Genesis and evolution of the 1997–98 El Niño. *Science*, **283**, 950–954.

Moron, V., R. Vautard, and M. Ghil, 1998: Trends, interdecadal and interannual oscillations in global sea-surface temperatures. *Climate Dyn.*, **14**, 545–569.

Rasmusson, E. M., and T. H. Carpenter, 1982: Variations in tropical sea surface temperature and surface wind fields associated with the Southern Oscillation/El Niño. *Mon. Wea. Rev.*, **110**, 103–1113.

Torrence, C., and G. P. Compo, 1998: A practical guide to wavelet analysis. *Bull. Amer. Meteor. Soc.*, **79**, 61–78.

Wang, B., 1995: Interdecadal changes in El Niño onset in the last four decades. *J. Climate*, **8**, 267–285.

Wang, B., and Y. Wang, 1996: Temporal structure of the Southern Oscillation as revealed by waveform and wavelet analysis. *J. Climate*, **9**, 1586–1598.

Yiou, P., D. Sornette, and M. Ghil, 2000: Data-adaptive wavelets and multi-scale SSA. *Physica. D*, **142**, 254–290.